

Comparative evaluation of performances of different conceptualisations of distributed HBV runoff response routines for prediction of hourly streamflow in boreal mountainous catchments

Teklu T. Hailegeorgis and Knut Alfredsen

ABSTRACT

Unidentifiability and equifinality of parameters pose challenges to calibration and prediction by conceptual precipitation-runoff models. Evaluation of prediction performances of parametrical parsimonious and more complex conceptualisations is lacking for hourly simulation. We conducted a comparative evaluation of four configurations of the distributed ($1 \times 1 \text{ km}^2$ grids) HBV (Hydrologiska Byråns Vattenballansavdelning) runoff response routines for hourly streamflow simulation for boreal mountainous catchments in mid-Norway. The routines include the standard Swedish Meteorological and Hydrological Institute HBV or HBV-SMHI, HBV-non-linear (standard soil routine and non-linear reservoirs), HBV-Soil Parsim R (standard soil routine and linear reservoirs) and HBV-Parsim (parsimonious and linear soil routine and reservoirs). The routines provided simulated hydrographs, flow duration curves and quantile–quantile plots, which are marginally different from each other for the study catchments. However, the HBV-Parsim provided better parameter identifiability and uncertainty, and simulated baseflow that better matches the baseflow separated by filtering techniques. Performances of the HBV-Parsim indicated a potential for application of parametrical parsimonious routines, which would benefit model updating for forecasting purposes. The study revealed strong effects of the soil moisture (SM) parameters on the recharge, percolation and hence the baseflow, which substantiates the importance of evaluating the internal simulation (e.g., SM and baseflow) of the HBV routines against measurements or analytical computations.

Key words | baseflow simulation, boreal mountainous catchments, distributed HBV runoff response routines, hourly runoff simulation, model calibration and spatio-temporal validation, parametrical parsimony

Teklu T. Hailegeorgis (corresponding author)
Knut Alfredsen
Department of Hydraulic and Environmental
Engineering,
NTNU,
NO-7491 Trondheim,
Norway
E-mail: tekhi09@gmail.com

INTRODUCTION

Various conceptual runoff response routines are currently used for decision-making for operational forecasting although they are not capable of detailed modelling of physical hydrological processes (e.g., preferential flows). Some of the recent works endorsing the utility of conceptual models include Fenicia *et al.* (2011) and Kavetski & Fenicia (2011) who tested a flexible framework for conceptual model structure for comparison and refinement of alternative hypotheses. Precipitation-runoff models based on the

standard HBV (Bergström 1976), which is named as the HBV-SMHI (Hydrologiska Byråns Vattenballansavdelning-Swedish Meteorological and Hydrological Institute) in the present study, and its variants have been widely applied in many countries for real-time forecasting of floods and inflow to storage reservoirs, for design flood estimation and for scenario studies such as the impacts of anticipated climate change (e.g. Harlin 1992; Harlin & Kung 1992; Killington & Sælthun 1995; Lindström 1997; Blöschl *et al.*

2008; Driessen *et al.* 2010). For the representation of spatial heterogeneity through different levels of spatial discretisation, the standard HBV model has evolved through different variants from lumped to ‘fully’ distributed versions (e.g., Lindström 1997; Beldring *et al.* 2003; Hundecha & Bárdossy 2004; Blöschl *et al.* 2008; Das *et al.* 2008; Li *et al.* 2014). Wrede *et al.* (2013) further implemented a ‘fully’ distributed HBV model complemented by subgrid scale parameterisation for distinct land use classes or hydrological response units for a Swedish lowland catchment. Based on the distributed model intercomparison project (DMIP) experiments, Smith *et al.* (2004) suggested distributed models as complements rather than replacements of the lumped models for operational forecasting purposes.

The HBV model has gained significant applications for daily forecasting, and with recent developments for hourly simulation/forecasting (e.g., Kobold & Brilly 2006; Shrestha & Solomantine 2008; Rakovec *et al.* 2012). There are growing interests in hourly application of the HBV model since hourly flood forecasting is becoming important due to the prevalence of extreme hydrological events driven by intense rainfall events. In addition, for operational hydropower management a reliable hourly inflow prognosis is required. For instance, real-time forecasting of inflow to hydropower reservoirs during hydropeaking (i.e., when hydropower is operating to balance intermittent renewables or non-renewable energy sources for peak demands of electricity) requires runoff simulation for shorter time steps for optimal scheduling and to minimise downstream impacts of releases. In addition, for catchments that are affected by diurnal variations of streamflow due to diurnal variations in snowmelt and evapotranspiration, the hourly simulation is expected to better capture the temporal dynamics of the hydrological processes for reliable prediction/forecasting of streamflow. Also, flood peaks may not be reliably simulated based on a coarse temporal resolution (e.g., daily time step) especially for small basins. Several studies have been conducted on time scale dependencies of conceptual model parameters (Littlewood & Croke 2008; Wang *et al.* 2009; Merz *et al.* 2009). Kavetski *et al.* (2011) thoroughly investigated the time scale dependencies of information content of data, parameter calibration and identifiability, quickflow and hydrograph peak simulation. The considerable loss in performance when parameters calibrated for a longer time step (e.g.,

daily streamflow) are used for simulation for a shorter time step (e.g., hourly), as demonstrated by Bastola & Murphy (2013), showed the introduction of additional uncertainty and hence associated risks in hourly prediction from utilising the daily calibrated parameters. Therefore, hourly predictions based on parameters calibrated utilising hourly observations are required for water management purposes.

Depending on their conceptualisation, the different versions of the HBV response routines contain different number of free parameters while large number of free parameters do increase the complexity in parameter calibration and identifiability. Moreover, the reliability of simulation based on different conceptualisation may be different. The standard form SMHI (Bergström 1976), the HBV light (Seibert 1997b, 2002) and the ‘Nordic’ HBV model (Sælthun 1996) all have two (non-linear upper and linear lower) reservoirs and three outlets (three recession coefficients, upper zone threshold and one percolation parameter). The operational HBV version used by Norwegian hydropower companies (Killingtveit & Sælthun 1995) has two (non-linear upper and linear lower) reservoirs and four outlets (four drainage coefficients, two upper zone thresholds and one percolation parameters). The HBV-96 (Lindström 1997) and the HBV-IWS (Hundecha & Bárdossy 2004) have two (non-linear upper and linear lower) reservoirs and four parameters (two recession coefficients, non-linearity exponent and percolation parameters). The van den Tillaart (2010) version of HBV contains two (non-linear upper and linear lower) reservoirs with five parameters (upper and lower reservoir recession coefficients, non-linearity exponent, percolation rate and capillary flux).

Reed *et al.* (2004) in the DMIP noted that model formulation and parameterisation could have a bigger impact on simulation accuracy than the spatial computational unit (lumped versus distributed). The authors also pointed out that due to interacting and compensating effects of different factors, studies based on changing one model component at a time will be required to identify reasons for any observed differences among the models. Parsimonious parameterisation is important since a large number of free parameters do not guarantee good model performance (e.g., Michaud & Sorooshian 1994). The cost of model calibration increases as the number of free parameters increases. The problem of equifinality and poor identifiability related to

overparameterisation, which potentially happens when complex models are calibrated using data of low information content, were addressed among others by [Beven & Binley \(1992\)](#), [Beven & Freer \(2001\)](#) and [Kirchner \(2006, 2009\)](#). [Werkhoven *et al.* \(2009\)](#) illustrated the importance of reduction of parameter dimensionality. Each additional parameter represents a whole new dimension of parameter space, so the overparameterisation problem grows with the number of free parameters ([Kirchner 2006](#)). [Uhlenbrook *et al.* \(1999\)](#) investigated the prediction uncertainty of different variants of the HBV model caused by problems in identifying model parameters and structure.

However, studies of relationships between prediction performances and various configurations of the distributed HBV response routines and the number of free parameters is lacking from the literature. Dependent on the ability of the model to simulate the precipitation–runoff relationships, conceptualisation based on less number of parameters is preferable. Despite the pros in allowing better identifiability of parameters, there are also cons against parsimonious models. For example, [Kuczera & Mroczkowski \(1998\)](#) noted that a simple model cannot be relied upon to make meaningful extrapolative predictions, where a complex model may have the potential but because of information constraints may be unable to realise it. Due to the pros and cons related to parsimony and more complexity in hydrological modelling, the focus of the present study is on comparative evaluation of the runoff response routines. Some of the previous attempts to reduce the number of free parameters in the HBV response routine include works by [Harlin \(1992\)](#) and [Winsemius *et al.* \(2009\)](#). [Samuel *et al.* \(2011\)](#) evaluated different configurations of the HBV response routines for baseflow simulation in Canada.

[Jakeman & Hornberger \(1993\)](#) in their ‘principle of parsimony’ claimed that simple conceptual models with four to five parameters provide an adequate fit if only streamflow is available for calibration. Observing a large degree of equifinality in calibration of the nine HBV-96 parameters for four climatologically different river basins, [Lidén & Harlin \(2000\)](#) stated that given the inherent limitations of information in calibration data only a smaller number of parameters can be uniquely identified which calls for a parsimonious model. When calibration is based on different

state variables (e.g., ground water level, soil moisture (SM), snow depth) in addition to streamflow, multi-objective calibration gives an opportunity to further exploit the information content of each variable to better constrain the model parameters. However, the challenge is that such a rich data set may not be readily available especially for operational purposes. Hence, the maximum possible exploitation of the information content of the relatively readily available streamflow data is a possible solution.

[Kokkonen & Jakeman \(2001\)](#) while explaining the higher information requirement of a complex model structure stated that the more process complexity one wants to include in the model structure the more types of data are required to estimate the process parameters and to test the model performance. [Perrin *et al.* \(2001\)](#) compared 19 lumped models for daily simulation in 429 catchments and found that models with a large number of parameters generally yield better calibration results, but were not verified in the validation stage. [Hughes \(2010\)](#) noted that if the model performance is evaluated only by the success of calibration against observed streamflow, certain simpler models would frequently out-perform the more complex models but selection of models for wider objectives such as prediction in ungauged basins is far more complex. Better process understanding augmented by field experiments and measurements to conceptualise improved (suitable) model structures for simulation of dominant hydrological processes is indispensable in catchment hydrology but this task was not an objective of the present study.

The main objective of the present study focuses on the evaluation of the performance of different configurations of the runoff response routine of the HBV model. The model configurations used in the study are the distributed ($1 \times 1 \text{ km}^2$) standard HBV (HBV-SMHI), non-linear storage–discharge relationships HBV (HBV-non-linear), standard SM accounting and linear parsimonious runoff response routine (HBV-Soil Parsim R) and parsimonious and linear conceptualisations of both the SM accounting and runoff response routines (HBV-Parsim). The main research questions are:

1. What are the performances of different configurations of the HBV runoff response routines for distributed ($1 \times 1 \text{ km}^2$) hourly runoff simulation in boreal mountainous

catchments in terms of prediction of various streamflow 'signatures', parameter identifiability and uncertainty?

2. What are the performances of the routines in terms of spatial and temporal validation when parameters are transferred to internal (interior) subcatchments and among the non-nested catchments inside the study watershed?

THE STUDY REGION

The study region is the mountainous boreal watershed of Gaula in mid-Norway. We used streamflow data from four stations, Gaulfoss, Eggafoss, Hugdal bru and Lillebudal bru. Hugdal bru, Eggafoss and Lillebudal bru are nested within Gaulfoss, but they are independent of each other. Rainfall mainly occurs from April to October, whereas snowfall occurs from November to March. We used hourly precipitation data from 12 climate stations with an elevation range from 127 to 885 masl (metres above sea level). We interpolated the climate inputs on the spatial computational scale of $1 \times 1 \text{ km}^2$ grids by the inverse distance weighing (IDW) method. The maximum length of input records for calibration was two years of hourly temporal scale due to difficulty in finding long series of hourly climate and streamflow data with complete records. However, the length of the hourly data series is expected to provide sufficient information on the rainfall-runoff relationships to constrain the model parameters. Where sub-daily data exist, it would appear to be wise to use the extra information they contain, leading to more accurate calibrated model parameters (Littlewood & Croke 2008).

The hourly climate data used include precipitation (P), temperature (T), wind speed (W_s), relative humidity (H_R) and global radiation (R_G). The main vegetation/land use types in the catchments are forests (conifers), upland and riparian areas. The dominant loose (soil) formation in the Gaula watershed is glacial tills underlain by impermeable bedrock geology (<http://www.ngu.no/no/hm/Kart-og-data>). The main surface deposits in the Nordic countries are till soils (Beldring *et al.* 2000). The main characteristics of the catchments and maps of land use, elevation, locations of climate and streamflow stations for the study catchments are given in Table 1 and Figure 1.

Table 1 | Main characteristics of the study catchments

Catchments	Gaulfoss	Eggafoss	Hugdal bru	Lillebudal bru
Catchment area, km^2	3,090	668	546	168
Hypsography (% of catchments below elevation, masl)				
0	54	285	130	516
20	534	717	503	770
40	663	811	583	907
60	813	878	664	983
80	945	964	816	1,045
100	1,330	1,284	1,256	1,330
Major soil types (%)				
Till soils (thick layer)	26.9	39.9	23.2	14.5
Till soils (thin layer)	33.0	27.8	38.7	29.5
Peat and marsh (organic material)	8.6	6.8	8.1	2.9
Bare mountains	24.0	23.9	20.1	49.1
Major types of bed rock geology (%)				
Gabbro and amphibolite	2.4	6.8	0.0	0.0
Amphibolite and schist	4.4	21.2	0.0	0.0
Greenstone and amphibolite	11.0	22.4	11.8	0.0
Quartzite	9.7	0.0	15.7	1.2
Mica gneiss, schist, amphibolite and metasandstone	48.2	8.7	41.3	97.7
Phyllite and schist	17.8	31.1	26.9	0.0
Major land use/cover classes (%)				
Farm land	2.7	2.1	6.0	0.5
Forest	36.7	24.6	53.6	21.7
Bare rocks/mountains above timber line	35.8	44.0	20.7	65.3
Marsh/bog	14.5	12.6	16.7	9.0
Lakes	2.1	2.8	1.0	1.1

MODELS AND METHODS

The four configurations of the conceptual HBV runoff response routines modelled and evaluated in the present study differ either in the number of conceptual reservoirs (one versus two), form of storage and discharge (S-Q) equations (linear versus non-linear), the SM accounting

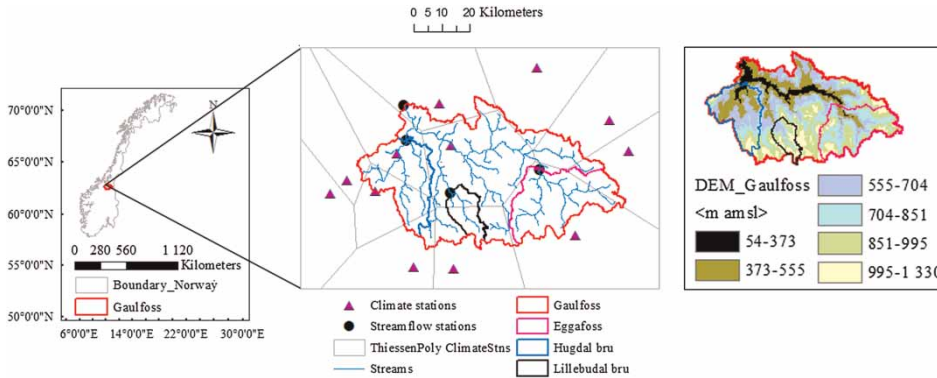


Figure 1 | Maps of location of the study catchments, hydroclimatic stations and elevation.

routine or the number of free parameters (few/parsimonious versus many/more complex). A summary of the main features of the routines is given in Table 2 and Figure 2. The lists of the free parameters and ranges of their uniform priors are given in Table 3.

The HBV-SMHI distributed runoff response routine

The distributed runoff response routine based on the standard HBV model used in the present study contains two conceptual reservoirs (Figure 2(a)). The upper reservoir contains two outlets (one with non-linear and one with linear drainage equations) and the lower reservoir is linear with only a single outlet. It has five free parameters in the response routine that include very quick and quick upper reservoir recession coefficients (k_2 and k_1 , respectively),

slow base flow recession coefficient (k_0), percolation rate (PERC) and upper reservoir threshold storage (UZ_t). For the upper reservoir, the runoff generated conceptually represents very quick and quick runoff components, both from overland flow and from groundwater drainage from perched aquifers (Killingtveit & Sælthun 1995). The storage–outflow relationship for the upper zone is threshold based and the total outflow from the upper reservoir (Q_{UZ}) is the sum of outflows from the lower (Q_{UZ1}) and upper (Q_{UZ2}) outlets. The lower zone conceptually represents the base flow from ground water and the storage–baseflow relationship is linear.

HBV-non-linear distributed runoff response routine

The HBV-non-linear runoff response routine has two storage reservoirs (upper and lower) conceptually similar to

Table 2 | Summary of the evaluated versions of the HBV-based SM accounting and runoff response routines. Calibrated parameters are shown in bold. The n_u and n_l are exponents of non-linearity for the upper and lower reservoirs, respectively

No.	Runoff response routines	Equations			No. of calib. soil + response parameters
		SM accounting	Outflow upper reservoir	Outflow lower reservoir	
1	HBV-SMHI	$R = I \times (SM/FC)^\beta$, AET/PET = SM/(LP × FC)	$Q_{UZ} = \max(0, \mathbf{k}_2 \times (UZ - UZ_t)) + (\mathbf{k}_1 \times \min(UZ, UZ_t))$, PERC	$Q_{LZ} = \mathbf{k}_0 \times LZ$	8
2	HBV-non-linear	$R = I \times (SM/FC)^\beta$, AET/PET = SM/(LP × FC)	$Q_{UZ} = \mathbf{k}_1 \times LZ^{n_u}$, PERC	$Q_{LZ} = \mathbf{k}_0 \times LZ^{n_l}$	8
3	HBV-Soil Parsim R.	$R = I \times (SM/FC)^\beta$, AET/PET = SM/(LP × FC)	$Q_{UZ} = \mathbf{k}_1 \times UZ$, PERC	$Q_{LZ} = \mathbf{k}_0 \times LZ$	6
4	HBV-Parsim	$R = I \times (SM/FC)$, AET/PET = SM/(LP × FC): LP = 0.9 & FC = 150 mm below timber line or 50 mm above	$Q_{UZ} = \mathbf{k}_1 \times UZ$, PERC	$Q_{LZ} = \mathbf{k}_0 \times LZ$	3

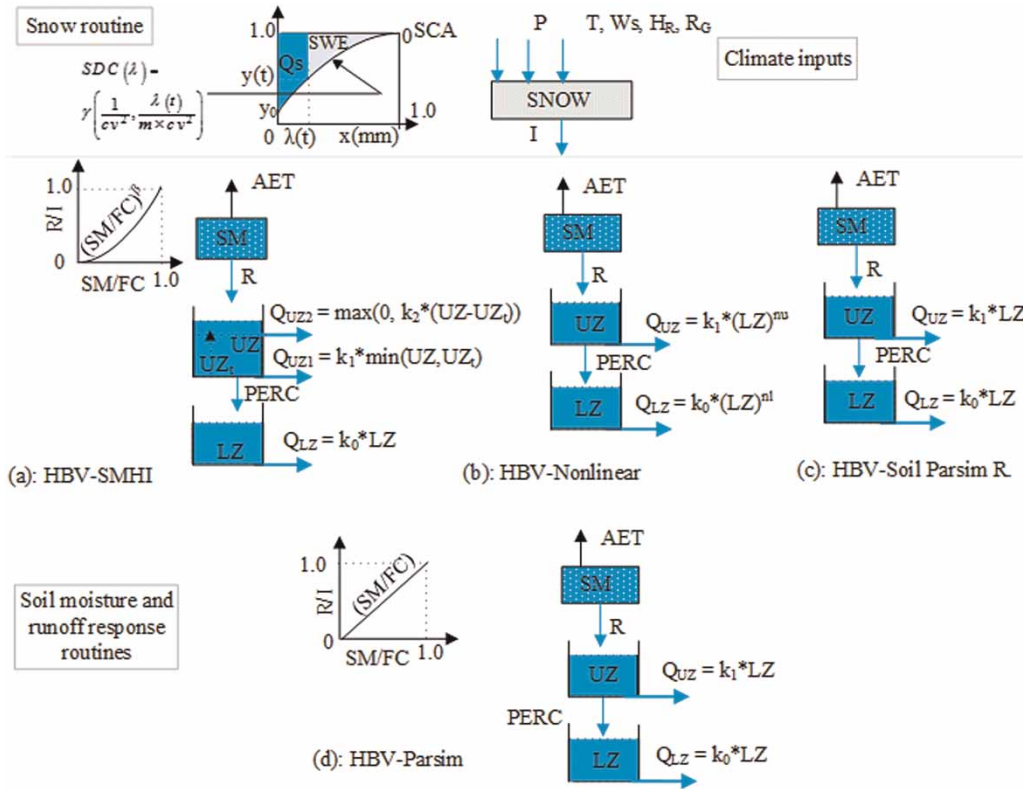


Figure 2 | Model structures (land grid cell): (a) HBV-SMHI, (b) HBV-non-linear, (c) HBV-Soil Parsim R and (d) HBV-Parsim. The snow routine is based on Kolberg & Gottschalk (2006).

Table 3 | Lists of calibrated (Calib.) parameters and their uniform prior ranges

No.	Calib. parameters	HBV-SMHI	HBV-non-linear	HBV-Soil Parsim R	HBV-Parsim	Units	Uniform prior range [Min, Max]
Snow							
1	TX	x	x	x	x	°C	[-3, 2]
2	WS	x	x	x	x	-	[1, 6]
SM accounting							
3	FC	x	x	x		mm	[50, 600]
4	LP	x	x	x		-	[0.7, 0.99]
5	β	x	x	x		-	[1, 5]
Runoff response							
6	k_2	x				d^{-1}	[0.005, 2.0]
7	k_1	x	x	x	x	d^{-1}	[0.001, 1.5]
8	k_0	x	x	x	x	d^{-1}	[0.0005, 0.5]
9	n_u		x			[-]	[0.2, 5]
10	n_l		x			[-]	[0.2, 5]
11	PERC	x	x	x	x	$mm\ d^{-1}$	[0, 6]
12	UZ_t	x				mm	[0, 80]

those of the HBV-SMHI routine but with the basic differences in configuration of the structure of the upper conceptual reservoir by a single outlet (Figure 2(b)) with an exponent based non-linear storage–outflow relationship and also a non-linear storage–baseflow relationship for the lower reservoir. The total number of parameters in the response routine is five (i.e., upper and lower reservoir recession coefficients, two non-linearity parameters and percolation). Simulation over fixed discrete time steps of the hourly data resolution was used in the present study assuming that the input forcings and fluxes are constant over the time step. The fixed-step approaches are commonly used for conceptual models (e.g., Lindström 1997; Blöschl *et al.* 2008). Focus on the effects of numerical artefacts (e.g., Clark & Kavetski 2010) in solving the storage–discharge functions was not the objective of the present study.

The HBV-Soil Parsim R distributed runoff response routine

The HBV-Soil Parsim R runoff response routine has two (upper and lower) reservoirs (Figure 2(c)) similar to those of the HBV-non-linear routine but with the basic differences that both the storage–outflow (upper reservoir) and storage–baseflow (lower reservoir) relationships are linear. Hence, the total number of parameters in the response routine are three, namely the quick reservoir recession coefficient (k_1), slow base flow recession coefficient (k_0) and percolation to the lower reservoir (PERC).

The HBV-Parsim distributed runoff response routine

The HBV-Parsim runoff response routine (Figure 2(d)) is similar to the HBV-Soil Parsim R response routine with the only difference in their SM accounting routines.

The SM accounting routine

The SM accounting routine partitions the effective precipitation into recharge to the upper zone and contribution to change in the SM storage. For the HBV-SMHI, HBV-non-linear and HBV-Soil Parsim R, the SM accounting is based on a non-linear function which partitions the infiltration from rainfall and snowmelt (I) into recharge (R) to upper

reservoir and change in SM storage or Δ_{SM} (Bergström 1976). The ‘non-linearity parameter’ β controls the shape of the partitioning curve. The SM storage is depleted by evapotranspiration. If the ratio of the actual SM to the field capacity (FC) or SM/FC exceeds the ‘limit for potential evaporation’ or evapotranspiration threshold parameter (LP), actual evapotranspiration (AET) is assumed to be equal to the potential evapotranspiration (PET). The FC represents the maximum SM holding capacity of the soil. However, if the SM is below (LP*FC), the AET decreases linearly with the decrease in SM storage (i.e., $AET/PET = SM/(LP*FC)$). Therefore, the SM accounting routine of the HBV-SMHI involves three free parameters, namely, the FC, shape parameter (β) and LP. A capillary flux (flow) from the storage reservoirs to the SM zone was not considered in the present study.

However, for the HBV-Parsim the SM accounting routine is based on a linear function (i.e., $\beta = 1.0$), LP is also set to a constant value of 0.9, which is a default value of HBV-96 (Booij 2005). The sensitivity of the HBV model to the FC parameter was studied by Seibert *et al.* (1997a), who reported both well-defined and badly-defined (i.e., insensitive or uncertain) cases, respectively, for some Swedish catchments and mountainous catchment in Germany. Abebe *et al.* (2010) found the FC parameter to be dominantly affecting the high flow and volume errors for semi-humid catchment in USA. Beldring *et al.* (2003) obtained FC values of 20–150 mm for different land cover from simultaneous calibration of a distributed version of the standard HBV model for 141 catchments in Norway. Following the results obtained by Beldring *et al.* (2003), we assigned field capacity values for different land classes due to our objective of testing a parametrical parsimonious response routine with a total number of five free parameters based on the ‘principle of parsimony’ by Jakeman & Hornberger (1993). For the Gaula watershed, land cover above timberline (approximate timberline elevation ranges from 800 to 850 masl) is mainly dominated by sparse vegetation, bedrock/cracked rock with some proportions of lichen, heather and shrubs. The area below the timberline is dominated by coniferous forests with some proportions of deciduous forests and non-forested areas such as farmland and marshes/bogs. Therefore, we used FC maps with values of 150 and 50 mm, respectively, below and above the timberline. Therefore, there is no free parameter in the SM

accounting routine (i.e., three free parameters are reduced compared to the HBV-SMHI, HBV non-linear and HBV-Soil Parsim R) routines.

The PET was computed using the Priestley–Taylor method (Priestley & Taylor 1972) for the all response routines:

$$\text{PET} = \alpha \frac{\Delta}{\Delta + \gamma} (R_n - G), \quad (1)$$

where α is the Priestley–Taylor constant, Δ is the slope of saturation vapour pressure curve at air temperature at 2 m (T2 m), γ is the psychrometric constant (0.67 hPaK^{-1}), R_n is the net radiation = net shortwave radiation (SR_n) + the net longwave radiation (LR_n). Priestley & Taylor (1972) obtained values of α , for diverse well-watered surfaces, between 1.08 and 1.34 with an overall mean of 1.26. Teuling *et al.* (2010) used $\alpha = 1.26$ for the Swiss catchment. Gardelin & Lindström (1997) determined the value of α by calibration. Following Teuling *et al.* (2010), we used an alpha value of 1.26 rather than calibrating the parameter due to our objective of testing parametrical parsimonious HBV model and due to expected less effect of fixing the parameter to an average value on the PET calculation for the snow-dominated boreal catchment. The SR_n is computed from the measured global radiation (R_G) and land albedo. The LR_n is computed based on Sicart *et al.* (2006). The soil/ground heat flux (G) = $(0.12) * R_n$ is assumed following Teuling *et al.* (2010).

If the grid cells are within a lake, direct precipitation on the lake, evaporation from the lake and outflow are considered for the lower reservoir zone (i.e., there is no SM accounting routine and the upper zone reservoir). The evaporation from the lake surface is assumed to be 40% above the potential evapotranspiration computed from the Priestley–Taylor method.

The snow routine

For the study catchments, snow accumulation and melt processes dominate during winter and spring seasons, respectively. Snow routines based on temperature index models or degree-day methods are commonly used to simulate snowmelt rates in many variants of the HBV models. However, in the present study, we used the gamma

distributed snow depletion curve or SDC, which uses radiation for surface layer energy and phase change calculations (Kolberg & Gottschalk 2006) for all the response routines. The routine uses a mass balance approach to simulate the melt water release (snowmelt runoff) from saturated snow (Q_s) and the remaining unmelted snow storage, the snow water equivalent (SWE) (Figure 2).

The snow depletion curve describes how the snow covered area (SCA) reduces gradually through the melt season by relating the fractional SCA in a grid cell to the mass balance of a heterogeneous snow cover (Kolberg & Gottschalk 2010). Kolberg & Gottschalk (2006, 2010) defined the four variables defining the snow pack state in a grid cell (Figure 2) as the average SWE or SWE (mm) at the start of melt season, the SWE coefficient of variation, cv (-), explaining the subgrid spatial heterogeneity, the fractional SCA at the melt start of the melt season (-) and the accumulated melt depth, λ (mm), aggregated from the melt season onset or end winter day. The free parameters in the routine are the TX, which is the snow–rain threshold temperature parameter and identifies the form of precipitation (rainfall or snow fall), and wind scale (WS), which is the snow melt sensitivity to the wind speed or wind turbulence driving heat fluxes. Details of the SDC-based snow routine can be found in Kolberg & Gottschalk (2006, 2010).

MODEL CALIBRATION

Different researchers (Harlin 1991; Lindström 1997; Seibert 1997a, 2000, 2003; Uhlenbrook *et al.* 1999; Hundecha & Bárdossy 2004; Bárdossy & Singh 2008; Das *et al.* 2008; Lawrence *et al.* 2009; Shrestha *et al.* 2009; Sorman *et al.* 2009; Abebe *et al.* 2010; Driessen *et al.* 2010; van den Tillaart 2010) applied various algorithms for parameter calibration and identifiability and uncertainty analyses for the HBV model.

In the present study, we used the DREAM (Differential Evolution Adaptive Metropolis) algorithm (Vrugt *et al.* 2009) implemented in ENKI hydrological modelling platform (Kolberg & Bruland 2012) for model calibration and assessment of parameter identifiability and uncertainty. To our knowledge, calibration of the HBV-based precipitation-runoff model by the DREAM algorithm had not been

pursued so far. In DREAM, multiple chains with different starting points in the parameter space run simultaneously for global exploration, and automatically tune the scale and orientation of the proposal distribution during the evolution to the posterior distribution (Vrugt & Ter Braak 2011). The calibration was performed based on a residual based log-likelihood (L-L) objective function:

$$\begin{aligned} \text{L-L} & \left(\delta / \sigma_{\varepsilon}^2, \sum_{t=1}^n \left(Q\text{sim}_t^{(\theta)} - Q\text{obs}_t^{(\theta)} \right)^2 \right) \\ & = \left(\frac{-n}{2} \log(2\pi) - \frac{n}{2} \log(\sigma_{\varepsilon}^2) - \frac{\sum_{t=1}^n \left(Q\text{sim}_t^{(\theta)} - Q\text{obs}_t^{(\theta)} \right)^2}{2\sigma_{\varepsilon}^2} \right) \times f, \end{aligned} \quad (2)$$

where $Q\text{sim}^{(\theta)}$ and $Q\text{obs}^{(\theta)}$, respectively, are the Box-Cox (Box & Cox 1964) transformed observed and simulated streamflow time series (t) of length n , δ represents the model parameters, θ is the Box-Cox transformation parameter, σ_{ε}^2 is the variance of error and f is a fraction of effectively independent observations. The logarithm form was used for simplicity and numerical stability and the function should adequately summarise the statistical properties of the residuals (Vrugt *et al.* 2013).

The Box-Cox transformation was performed in order to obtain an approximately normal distributed series with homoscedastic residuals (i.e., variance of residuals is independent of streamflow). Homoscedasticity in the residuals provides an advantage in that the model residuals can be represented by one single distribution, most often Gaussian (Willems 2009). If $\theta = 0.0$ (log-transformation), it corresponds to an assumption of lognormal distributed streamflow and it gives high weights to low flows like the Nash-Sutcliffe efficiency (Nash & Sutcliffe 1970) for a log-transformed data (NSELn). If $\theta = 1.0$ (no transformation), it is assumed that the streamflow series is Gaussian and weight of high flows will be much greater than low flows like the Nash-Sutcliffe efficiency or NSE. The main advantage of the DREAM algorithm is that it accepts better parameter proposals (i.e., higher likelihood) and converges to posterior distributions rather than to a single optimal parameter set and allows an objective assessment for parameter identifiability and predictive uncertainty. We used the last 50% of the DREAM accepted marginal posterior parameters

after the burn-in iterations (Vrugt *et al.* 2009) for the evaluation of parameter identifiability, correlation and presentation of minimum and maximum ranges of posterior parameters. However, for a 'fit for purpose' evaluation of the routines in terms of their maximum performance in simulating the hydrographs, we picked the optimal parameter sets which correspond to the maximum values of the NSE and NSELn performance measures among the whole accepted by the DREAM algorithm. Burn-in iteration refers to discarding an initial portion of the samples to minimise the effect of initial conditions.

Values of θ from 0.25 to 0.3 are commonly used in the literature (e.g., Vrugt *et al.* 2002 and references therein; Willems 2009). However, in the present study, θ values of -0.14 , -0.1 , 0.05 and -0.35 , respectively, for Gaulfoss, Eggafoss, Hugdal bru and Lillebudal bru were estimated/optimised from the hourly observed streamflow series based on the 'fminsearch' optimisation algorithm in Matlab software. The algorithm calls for finding the θ value that maximises a log-likelihood function (<http://www.mathworks.com>). Box & Cox (1964) also proposed a maximum-likelihood method for estimation of θ that satisfies a normal distributed and homoscedastic transformed series. Details on how the 'fminsearch' optimisation algorithm works can be found from <http://www.mathworks.com>. Optimising the Box-Cox transformation provides as close as normal distributed series and homoscedastic residuals, but when the objective of simulation focuses on prediction of high flows, it may be preferable to use higher values of θ (for instance, $\theta = 0.3$ is common in the literature). We used the same transformation for all the compared runoff response routines and this specific issue related to selection of θ was not our focus in the present study.

The fraction of effectively independent observations f was introduced to address problems related to correlation of residuals. The amount of information obtained from the data is much less than the nominal number of observation suggests due to a serial correlation (independence) in the hourly streamflow series. Setting the f value to 1.0 implies the observations are considered independent. We computed the fraction of effectively independent observations from the autoregressive or AR (1) model of error covariance (Zięba 2010). Further details of the DREAM algorithm can be found in Vrugt *et al.* (2009).

POST-CALIBRATION ANALYSES (COMPARATIVE EVALUATION)

Model validation aims to validate the model's robustness and ability to describe the catchment's hydrological response, and further detect any biases in the calibrated parameters (Gupta *et al.* 2005). A set of calibrated model parameters are expected to provide reasonable performance when transferred in time to a separate data set for the same catchment. We used the split sample test (Klemeš 1986) for temporal validation of the routines and the proxy basin test for spatial transfer of parameters to 'proxy ungauged' catchments (for spatial validation). We also transferred the parameters in both space and time for spatio-temporal validation of the routines.

Transferability of model parameters in space and consistency of model performance for multi-sites for the internal subcatchments builds our confidence of the predictive performance of the model. The main objective of transferring parameters to other catchments within the watershed in the present study is for spatio-temporal validation of the model and to test the possibility of simulating at interior locations based on parameter set calibrated for the streamflow at the catchment outlet that was one of the research questions by the DMIP (Smith *et al.* 2004). We comparatively evaluated the routines based on transferability of their respective calibrated parameter set to 'proxy ungauged' internal or neighbouring catchments within the study watershed. Transfer of calibrated parameters to another watershed in the region for prediction in ungauged basins (PUB) was not an objective in the present study due to the limited number of catchments. In addition, study on the effects of land use and climate change was not an objective due to limited length of data. The NSE and NSELn performance measures were used for evaluations as discussed earlier. We used the parameter sets among the whole calibration that correspond to maximum values of the NSE and NSELn for comparisons of observed versus simulated hydrographs and to test temporal and spatial transferability of parameters within the watershed.

Different frameworks for assessment and quantification of parameter identifiability and uncertainty are available in the literature (see Uhlenbrook *et al.* 1999; Wagener *et al.*

2005; Pechlivanidis *et al.* 2011; Vrugt & Ter Braak 2011). Uhlenbrook *et al.* (1999) used plots of objective function versus the parameters and Vrugt & Ter Braak (2011) used plots of posterior density of the parameters to assess parameter identifiability and uncertainty. In this work, plots of posterior parameters versus corresponding L-L objective function and linear correlation coefficient matrix of the posterior parameters (Moreda *et al.* 2006; Schoups & Vrugt 2010) were presented to express parameter identifiability and uncertainty. The DREAM calibration algorithm converges as the Gelman–Rubin convergence (Gelman & Rubin 1992) comes below 1.2. Therefore, it is not prone to subjective fixing of the number of simulations, which is one of the limitations of the pure Monte Carlo (MC) calibration methods. Among the whole DREAM generated and evaluated parameter sets, we filtered the parameter vectors that are accepted by the DREAM algorithm. As discussed earlier, we used the last 50% of the DREAM accepted marginal posteriors after the burn-in iterations for parameter identifiability and uncertainty.

RESULTS

Observed versus simulated streamflow hydrographs for Gaulfoss from parameter sets corresponding to the maximum NSE are presented in Figures 3(a) and 3(b). Simulated baseflow from parameter sets corresponding to the maximum NSE and NSELn performance measures are presented in Figures 3(b) and 3(c), respectively. The simulated baseflow index (BFI), which is the ratio of simulated baseflow to the simulated streamflow is given in Table 4 for Gaulfoss and Eggafoss. For spatial and temporal validation of the model through transfer of calibrated parameters in space (among internal and neighbouring catchments inside the Gaulfoss watershed) and also in time, maximum NSE/NSELn values for the calibrated catchments corresponding to the calibrated (optimal) parameter sets and the NSE/NSELn values obtained from transfer of the calibrated parameter sets to 'proxy ungauged' catchments are given in Table 5.

The observed and simulated streamflow hydrographs showed satisfactory agreements (Figure 3(a) and 3(b) for

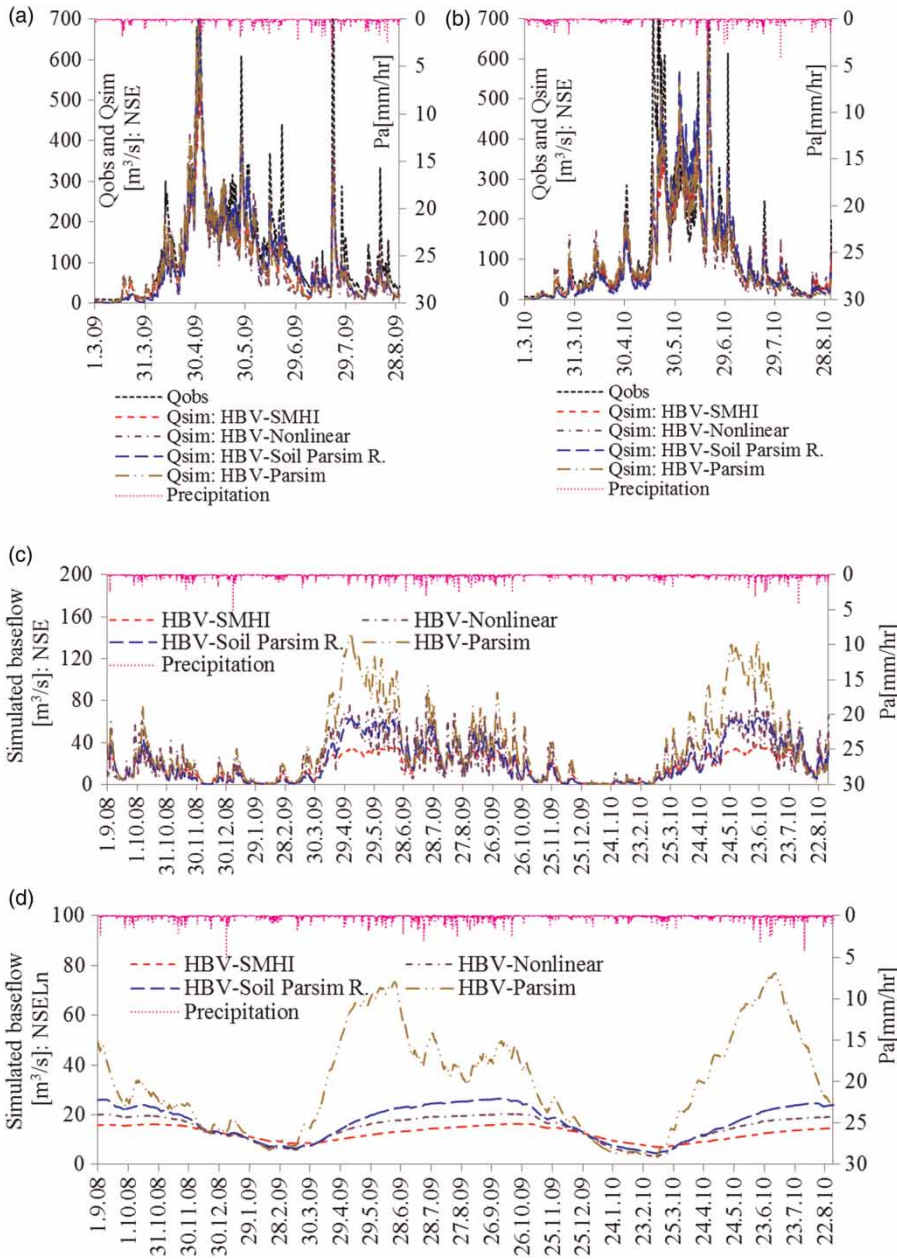


Figure 3 | (a) and (b) Simulated and observed streamflow hydrographs for Gauffoss for part of calibration period, and baseflow hydrographs for Gauffoss for the calibration period corresponding to (c) NSE and (d) NSELn. The Pa is an IDW interpolated and catchment averaged precipitation.

Table 4 | BFI from simulated streamflow and baseflow for calibrated parameter sets corresponding to maximum NSE/NSELn for Gauffoss and Eggfoss catchments (2008–2011)

Catchment	HBV-SMHI	HBV-non-linear	HBV-Soil Parsim R	HBV-Parsim
Gauffoss	0.29/0.21	0.41/0.25	0.37/0.29	0.62/0.55
Eggfoss	0.64/0.34	0.39/0.25	0.44/0.25	0.70/0.52

Gauffoss) for three of the four catchments. For Gauffoss, Eggfoss and Hugdal bru, the NSE/NSELn performance measures corresponding to the calibrated parameters range from 0.68 to 0.87, the NSE/NSELn for spatially and spatio-temporally transferred parameters range from 0.65 to 0.84 and from 0.47 to 0.90, respectively (Table 5). The

Table 5 | The NSE/NSELn performance measures for the calibrated and transferred in space and time (spatial and temporal validation) parameter sets

Calibrated catchment	Calibration and validation (2008–2010), (2010–2011 for Hugdal)				Validation (2010–2011)		
	'Proxy ungauged' catchments (internal or neighbouring catchments)						
	Gaulfoss	Eggafoss	Hugdal	Lillebudal	Gaulfoss	Eggafoss	Lillebudal
HBV-SMHI							
Gaulfoss	0.74/0.87	0.68/0.83	0.68/0.77	0.41/ – 1.89	0.72/0.88	0.49/0.82	– 0.05/ – 1.99
Eggafoss	0.69/0.83	0.68/0.86	0.66/0.79	0.11/ – 1.74	0.65/0.85	0.47/0.84	– 0.02/ – 2.91
Hugdal	0.74/0.74	0.68/0.71	0.69/0.87	0.39/ – 3.54	0.71/0.84	0.49/0.80	– 0.05/ – 4.00
Lillebudal	0.72/0.44	0.66/0.23	0.51/ – 1.33	0.42/0.45	0.70/0.60	0.52/0.49	– 0.05/ – 0.50
HBV-non-linear							
Gaulfoss	0.75/0.85	0.71/0.83	0.72/0.76	0.43/ – 2.49	0.71/0.89	0.52/0.85	– 0.03/ – 3.12
Eggafoss	0.71/0.84	0.69/0.85	0.69/0.79	0.43/ – 1.57	0.68/0.87	0.50/0.84	– 0.01/ – 2.50
Hugdal	0.72/0.79	0.69/0.84	0.69/0.86	0.43/ – 3.00	0.69/0.85	0.49/0.81	– 0.02/ – 3.97
Lillebudal	0.72/0.25	0.67/0.02	0.75/0.43	0.43/0.45	0.66/0.38	0.50/0.28	– 0.02/ – 0.66
HBV-Soil Parsim R							
Gaulfoss	0.75/0.86	0.65/0.84	0.67/0.78	0.41/ – 1.71	0.73/0.90	0.48/0.86	– 0.07/ – 2.44
Eggafoss	0.73/0.84	0.70/0.87	0.66/0.82	0.41/ – 1.54	0.69/0.87	0.50/0.85	– 0.02/ – 2.51
Hugdal	0.70/0.74	0.66/0.81	0.67/0.87	0.40/ – 3.78	0.68/0.82	0.49/0.80	– 0.04/ – 4.61
Lillebudal	0.71/0.32	0.69/0.27	0.70/0.52	0.41/0.40	0.70/0.41	0.49/0.41	– 0.04/ – 0.52
HBV-Parsim							
Gaulfoss	0.75/0.83	0.71/0.84	0.71/0.79	0.43/ – 2.64	0.71/0.85	0.50/0.84	– 0.03/ – 3.78
Eggafoss	0.70/0.81	0.70/0.86	0.68/0.79	0.42/ – 2.31	0.66/0.81	0.47/0.81	– 0.00/ – 3.51
Hugdal	0.77/0.72	0.71/0.80	0.74/0.83	0.43/ – 4.44	0.74/0.77	0.52/0.79	– 0.05/ – 5.44
Lillebudal	0.73/0.71	0.68/0.28	0.70/0.44	0.43/0.34	0.72/0.75	0.49/0.47	– 0.05/ – 0.74

The bold values correspond to calibrated parameters.

Hugdal = Hugdal bru; Lillebudal = Lillebudal bru.

NSE values for the calibration period for Eggafoss could be raised to 0.70 (only by an order of 0.02) by choosing a higher Box–Cox transformation parameter (i.e., $\theta = 0.3$, which is common in the literature) rather than optimising it. Low NSE performances for Eggafoss for the split sample tests may be attributed to the effects of unrepresentativeness or low quality hydroclimatic data for the validation period.

For further comparative evaluations, reliability of predictions is presented for Gaulfoss in Figures 4(a)–4(d) in terms of quantile–quantile (QQ) plots to test the consistency of the predictive distribution and the observed data (Kavetski & Fenicia 2011). We presented the QQ plots in terms of the empirical cumulative distribution functions or probability of non-exceedance of the observed and simulated streamflow, and departures of the plots from the

theoretical uniform distribution (i.e., the 1:1 diagonal line) indicate the discrepancy between the predictive distribution and the observed data (Figures 4(a)–4(d)). In addition, we further evaluated the routines for their performance in simulating the temporal variability of streamflow in terms of flow duration curves (FDCs) (Figure 5).

Table 5 shows the results of split-sample tests (temporal validation), 'proxy ungauged' basin test (spatial-validation) and spatio-temporal transfer of parameters among the four catchments in the Gaulfoss watershed. The DREAM calibrated parameter sets corresponding to the maximum NSE for the Gaulfoss catchment were validated for temporal, spatial and spatio-temporal transferability. Spatial validation and spatio-temporal validation for Eggafossen and Hugdal bru (when parameters are transferred to Gaulfoss

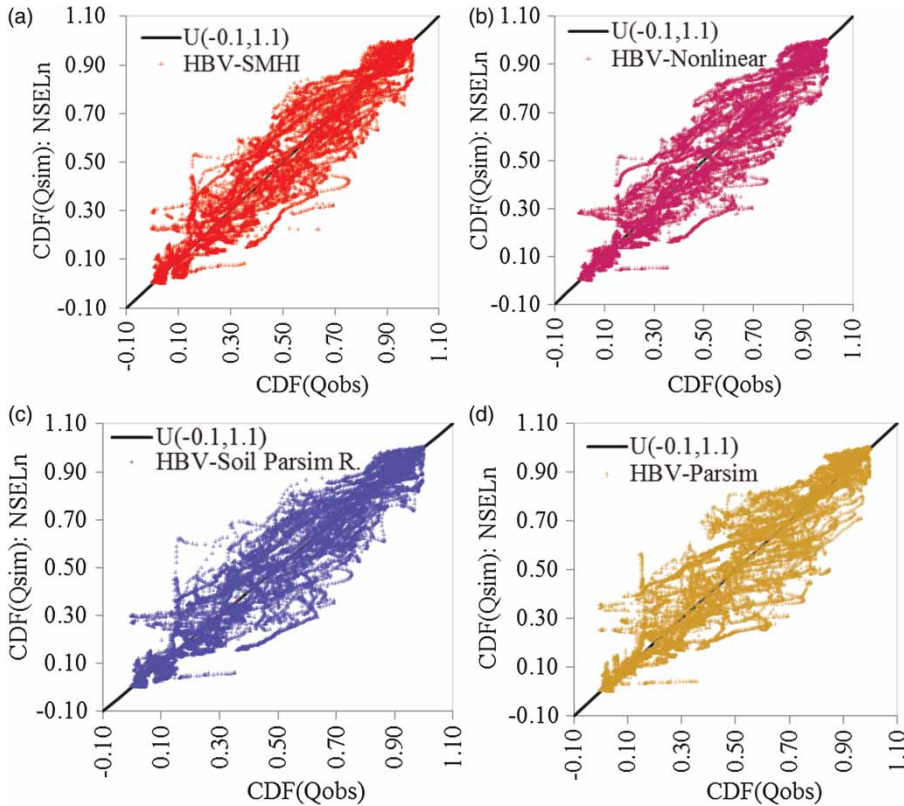


Figure 4 | Q-Q plots for observed versus simulated flows for parameter set corresponding to maximum NSELn for Gaulfoss: (a) HBV-SMHI, (b) HBV-non-linear, (c) HBV-Soil Parsim R and (d) HBV-Parsim.

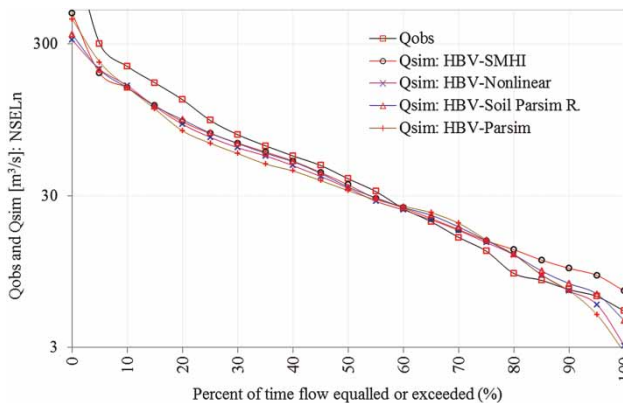


Figure 5 | Observed versus simulated FDCs for parameter set corresponding to maximum NSELn for Gaulfoss.

catchment) also performed well although temporal validation for Eggfossen resulted in less performances. Good quality streamflow data were available only from 2010 to 2011 for Hugdal bru catchment and hence we did not

perform temporal validation for the catchment. However, calibration and temporal validation for the smallest catchment (Lillebudal bru) resulted in low performance measures. The spatio-temporal transfer of calibrated parameters for Lillebudal bru provided better results for the NSE performance measures, although it gave very poor performances for the NSELn (low flows). Lillebudal bru catchment is dominated by a mountainous topography (Figure 1) where large portions of the catchment are at elevations above the climate stations from which data were used in the present study. In addition, the precipitation stations are far from Lillebudal catchment and hence their representativeness for spatially interpolated areal precipitation fields may be low. We also tested the effects of the quality of streamflow data for Lillebudal bru by calibrating the routines for the validation data (2010–2011) but the result showed no improvement in the calibration performances. Nevertheless, contingent on the quality and representativeness of input climate data, calibration of the

conceptual HBV runoff response routines provided predictions which were validated by transferability of parameter sets in space and time to the internal (interior) and nearby 'proxy ungauged' catchments.

We present the results of the DREAM L-L calibration in terms of plots of posterior parameters versus the L-L objective function in Figures 6(a)–6(d) for Gaulfoss to evaluate parameter identifiability from the last 50% of the DREAM accepted parameter vectors after the burn-in iterations until the DREAM converges. The number of simulations (iterations) plotted are 3,223 (Figure 6(a)), 3,411 (Figure 6(b)), 2,857 (Figure 6(c)) and 914 (Figure 6(d)) for the HBV-SMHI, HBV-non-linear, HBV-Soil Parsim R and HBV-Parsim, respectively. Ranges of the prior and posterior parameters, and optimal parameters corresponding to maximum NSE and NSELn are given in Table 6. The linear correlation

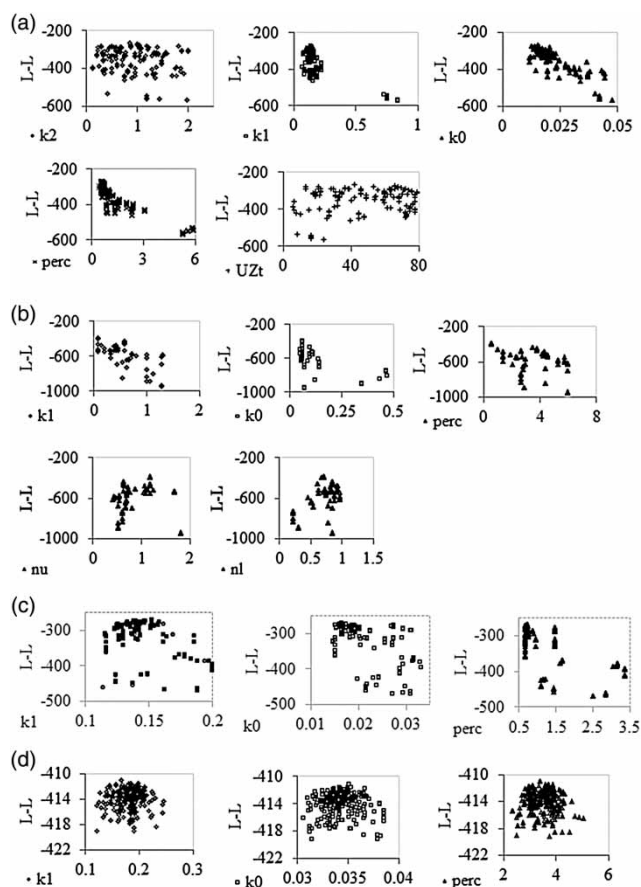


Figure 6 | Identifiability of the posterior runoff response parameters from the DREAM calibration for Gaulfoss: (a) HBV-SMHI, (b) HBV-non-linear, (c) HBV-Soil Parsim R and (d) HBV-Parsim. The L-L is the log-likelihood function.

matrix among the posterior parameters in the SM accounting and runoff response routines for Eggafoss catchment is presented in Table 7.

DISCUSSION

A comparative evaluation of parsimonious versus more complex configurations of distributed conceptual HBV response routines was performed in terms of prediction of different runoff 'signatures' (hydrographs, FDCs and baseflow), spatial and temporal validation of the routines and parameter identifiability and uncertainty. The results indicated that there are only marginal differences among the total streamflow predictions by the parsimonious and more complex routines. It complies with the advantages of the 'principle of parsimony', which was illustrated by Jake-man & Hornberger (1993). However, by testing the internal simulation of the routines in terms of the baseflow, we could observe differences in performances among the routines in simulation of the baseflow contributions to the streamflow.

Simulated hydrographs, baseflow, QQ plots and FDCs

Plots of simulated streamflow hydrographs corresponding to the maximum NSE performance measure (Figures 3(a) and 3(b)) versus the observed streamflow hydrograph indicated only marginal differences in the performances of the routines in terms of reproducing the time series of streamflow. All the four cases of conceptualisation of the routines gave low simulated streamflow (Q_{sim}) compared to the observed streamflow (Q_{obs}) during summer high flow events. The SM routine parameters particularly influence the discharge volume and the fast flow routine parameters particularly affect the shape of the hydrograph and extreme discharges (Booij 2005). Abebe *et al.* (2010) noted the FC as a dominant parameter affecting both high flow series and runoff volume. In the SM accounting routine, the FC and the evapotranspiration threshold parameter (LP) control the amount of evapotranspiration while β controls partitioning of infiltration (I) into recharge to the upper reservoir (R) and change in SM (Δ_{SM}). At any relative saturation (SM/FC) of the SM zone, a larger proportion of the infiltrated water

Table 6 | Ranges of prior, posterior and optimal (corresponding to maximum performance measures NSE and NSELn) response routines parameters for Gaulfoss and Eggafoss

Parameters	Uniform prior		Gaulfoss				Eggafoss			
	Min	Max	Posterior		Optimal		Posterior		Optimal	
			Min	Max	NSE	NSELn	Min	Max	NSE	NSELn
HBV-SMHI										
k_2	0.005	2	0.13	1.99	1.14	0.99	0.05	2.00	1.08	0.54
k_1	0.001	1.5	0.06	0.83	0.53	0.14	0.04	0.45	0.82	0.22
k_0	0.0005	0.5	0.01	0.05	0.38	0.01	0.03	0.22	0.27	0.03
PREC	0	6	0.45	5.88	0.96	0.49	0.00	5.28	4.12	1.00
UZ_t	0	80	5.51	78.78	39.70	58.73	1.94	79.20	18.44	25.20
HBV-non-linear										
k_1	0.001	1.5	0.07	1.30	1.00	0.07	0.01	1.33	0.96	0.30
k_0	0.0005	0.5	0.04	0.47	0.43	0.06	0.00	0.49	0.23	0.04
PREC	0	6	0.57	5.96	1.97	0.57	0.62	5.98	1.78	0.62
n_u	0.2	5	0.42	3.65	0.91	1.16	0.48	2.31	0.86	0.86
n_l	0.2	5	0.21	4.10	2.11	0.71	0.20	2.25	0.75	0.80
HBV-Soil Parsim R										
k_1	0.001	1.5	0.11	0.20	0.56	0.19	0.07	0.54	0.76	0.18
k_0	0.0005	0.5	0.01	0.03	0.34	0.02	0.02	0.07	0.44	0.03
PREC	0	6	0.65	3.37	1.81	0.76	0.42	5.69	1.79	0.59
HBV-Parsim										
k_1	0.001	1.5	0.12	0.25	0.71	0.24	0.07	0.57	0.72	0.29
k_0	0.0005	0.5	0.03	0.04	0.30	0.04	0.03	0.06	0.44	0.05
PREC	0	6	2.36	5.06	4.46	2.58	0.84	5.96	5.65	2.27

will replenish the SM zone as β increases. However, the non-linear effect of varying soil saturation becomes more pronounced for larger β and there is a rapid increase in the amount of infiltrated water that recharges the upper zone reservoir as relative saturation increases. However, the HBV-SMHI routine, which has three free parameters in the SM accounting routine (FC, LP and β) and also the very quick recession coefficient (k_2) in the response routine shows no marked better performance for simulation of high flows during summers. Although it does not contain the very quick runoff component, the simulated peak flow from HBV-Parsim was indistinguishable from those of the other routines. These findings may indicate compensation effects among model parameters, the crucial importance of the quality of input precipitation data to improve simulation of peak events and the potential for equivalent performances of the parsimonious routines.

The main reasons for lower simulated peak flow during summer periods may be attributed to less representativeness of the input precipitation data, particularly in capturing intense localised rainfall events. In addition, low quality streamflow data especially during flood events may contribute to the problem. The effect of Box-Cox transformation for simulation of high flows was checked for Eggafoss catchment but only an increase of NSE values by 0.02 were obtained for $\theta = 0.3$. The conceptual nature of the model structures could also be another explanation. Uncertainty due to parameter estimation and model structure alone cannot address the uncertainty in the prediction and hence assessments of uncertainties in the input data need to be included to improve decision-making under uncertainty.

Also, prediction based on the NSELn performance measure that gives higher weightage to the low flows are indistinguishable for the three configurations (Table 5).

Table 7 | Linear correlation matrix among the posterior response routine parameters for Eggafoss

HBV-SMHI	FC	LP	B	k_2	k_1	k_0	PERC	UZ _t
FC	1.00	-0.13	0.43	-0.04	-0.46	-0.14	-0.75	0.19
LP		1.00	-0.02	0.09	0.13	0.03	0.00	-0.12
B			1.00	0.01	-0.08	-0.37	-0.20	0.12
k_2				1.00	0.42	-0.24	0.23	0.49
k_1					1.00	-0.33	0.71	0.34
k_0						1.00	-0.09	-0.33
PERC							1.00	-0.08
UZ _t								1.00
HBV-non-linear	FC	LP	B	k_1	k_0	PERC	n_u	n_l
FC	1.00	-0.08	0.27	-0.56	0.19	-0.22	0.63	0.19
LP		1.00	-0.03	-0.05	-0.28	0.14	-0.09	0.12
B			1.00	-0.21	0.07	0.11	0.09	-0.22
k_1				1.00	-0.28	0.32	-0.71	0.03
k_0					1.00	-0.56	0.33	-0.75
PERC						1.00	-0.18	0.44
n_u							1.00	0.18
n_l								1.00
HBV-Soil Parsim R	FC	LP	B	k_1	k_0	PERC		
FC	1.00	-0.01	0.21	-0.15	-0.32	-0.57		
LP		1.00	0.00	0.01	-0.10	-0.15		
B			1.00	0.01	0.23	0.19		
k_1				1.00	0.37	0.52		
k_0					1.00	0.74		
PERC						1.00		
HBV-Parsim	k_1	k_0	PERC					
k_1	1.00	0.34	0.68					
k_0		1.00	0.49					
PERC			1.00					

Absolute correlation coefficients $|r|$ of >0.6 are shown in bold.

However, in terms of the quantity of simulated baseflow from the lower (ground water) reservoir, the HBV-Parsim provided considerably high contribution of baseflow (Figures 3(c) and 3(d)) based on both performance measures compared to the HBV-SMHI, HBV-non-linear and HBV-Soil Parsim R. Simulated BFI corresponding to the maximum NSE/NSELn performance measures for the HBV-Parsim are 0.62/0.55 and 0.70/0.52 for Gaulfoss and Eggafoss, respectively (Table 4). However, BFI values of greater than 0.8 were estimated from observed streamflow based on a Web-based Hydrography Analysis Tool (WHAT) baseflow separation of

the United States Geological Survey (Lim *et al.* 2005), but the validity of the filtering equations and parameters in 'WHAT' for the boreal catchments needs further study. Also, previous studies such as Beldring *et al.* (2000 and references therein) reported significant groundwater contribution to the total streamflow for boreal/humid temperate catchments. Therefore, the HBV-Parsim presumably provided reliable simulation of baseflow, but a tailor-made study is required on suitable baseflow separation techniques (e.g., Willems 2009) for the boreal catchments, which was not an objective in the present study.

The HBV-Parsim and HBV-Soil Parsim R have similar linear storage-outflow and storage-baseflow model structure in their response routines but differs in their SM accounting routines, i.e., the latter is based on the SM accounting routine of Bergström (1976). Therefore, the differences in the baseflow simulation results of the HBV-Parsim are most likely related to its parsimonious parameterisation of the SM accounting routine. Abebe *et al.* (2010) found the strong effects of the SM accounting parameters on the runoff volume and the FC as a dominant parameter affecting both high flow series and runoff volume. The present study showed a strong negative correlation between the FC and percolation parameter (PERC) (Table 7). The marked negative correlation between FC and PERC is due to a decrease in the recharge to the upper reservoir as FC increases or relative saturation decreases. Reduced recharge results in reduced percolation rate. This reduction in percolation rate, in turn, potentially decreases the baseflow contribution, which was observed for the three routines with the FC as a free calibration parameter. Samuel *et al.* (2011), based on the SM accounting routine of Bergström (1976), found that the configuration, which is similar to the HBV-SMHI but with non-linear storage–discharge relationships in the lower reservoir outperformed for baseflow simulation those configurations which are the same as the HBV-SMHI and HBV-non-linear. The authors used the Thornthwaite method for computation of potential evapotranspiration and the recursive digital filter for separation of baseflow from observed streamflow series (for comparison against the simulated baseflow) based on the assumption of filtering out high-frequency signals (quick flow) to separate low-frequency baseflow (Nathan & McMahon 1990).

The conceptual very quick flow from the upper outlet of the upper reservoir (Q_{UZ2}) for the HBV-SMHI corresponding to the optimal parameters for NSE and NSELn for Gaulfoss and Eggafoss range from 0.30 to 17% of the total simulated streamflow which showed slight exceedance of the threshold in the upper reservoir and a small proportion of the very quick flow contributing to the total streamflow. Figure 6 shows less identifiability of the threshold parameter (UZ_t), which may be related to its low sensitivity and hence its influence on the other parameters is not clearly observed.

The QQ plots for evaluating the reliability of prediction indicated significant over and under predictions from low to high ranges of streamflow that are indistinguishable among the four runoff response routines (Figures 4(a)–4(d)). There are also similar marginally different performances in prediction of FDCs which are mainly characterised by underestimation of high flows for all of the routines (Figure 5). Therefore, further evaluations based on additional runoff ‘signature’ and reliability criteria also do not suggest any clear superiority of the more complex routines.

Model validation (temporal, spatial and spatio-temporal)

Testing whether the distributed models that are calibrated with basin outlet streamflow information provide meaningful hydrologic simulation at internal catchments was one of the scientific questions tested by the DMIP (Smith *et al.* 2004). In the present study, marginal better performances from transfer of parameters from Gaulfoss to its internal catchments Eggafoss and Hugdal bru were observed for the HBV-non-linear and HBV-Parsim routines (NSE from 0.71 to 0.72 and NSELn from 0.76 to 0.84; Table 5). Therefore, calibration results of the distributed routines indicated the possibility for hourly prediction also at ungauged interior locations within the watershed through transfer of parameters. For some of the routines, equivalent or slight improvements in the NSE for the transferred parameter set from the watershed outlet (Gaulfoss) than the explicit local calibration at the interior locations of Eggafoss and Hugdal bru occurred, probably due to the differences in the representativeness of climate stations and hence the accuracy of areal precipitation, and the quality of streamflow data used for the model calibration. Both spatial transfer of parameter sets and explicit calibration performed poorly for the smallest catchment of Lillebudal bru especially for NSELn (gives weightage for simulation of low flow). Less performance in low flow may also indicate less performance in simulation of baseflow that may also suggest problems with stage–discharge curve during low flows at Lillebudal and subsurface peculiarities of Lillebudal catchment in addition to the less representative precipitation input.

Parameter identifiability and uncertainty

Figures 6(b)–6(d) show maximum L-L objective function for narrow ranges of parameters of the HBV-non-linear, HBV-Soil Parsim R and HBV-Parsim response routines. There is better likelihood of obtaining narrow predictive uncertainty of streamflow from posterior parameters yielding narrow maximum objective function. However, for the HBV-SMHI with ten free parameters the posterior ranges of parameters in the threshold-based non-linear upper reservoir k_2 and UZ_t (Figure 6(a)) are not much narrower than their corresponding uniform prior ranges (Table 6) which indicate their poor identifiability. Uhlenbrook *et al.* (1999) attributed the non-identifiability of parameters to uncertainty in model parameters or lack of sensitivity of model output to the change in parameters. Therefore, prediction uncertainty of a response routine with insensitive and unidentifiable parameters is expected to be high.

Narrower ranges of posterior parameters compared to the prior ranges for the HBV-Soil Parsim R and the HBV-Parsim compared to the others indicated less parameter uncertainty for the parsimonious runoff response routines (Table 6). For instance, for the HBV-Soil Parsim R routine for maximum NSE for the Gaulfoss catchment, the posterior ranges of k_1 (0.11–0.20), k_0 (0.01–0.03) and PERC (0.65–3.37) were obtained. Also, for the HBV-Parsim routine for maximum NSE of the Gaulfoss catchment, the posterior ranges of k_1 (0.12–0.25), k_0 (0.03–0.04) and PERC (2.36–5.06) were obtained. The uniform prior ranges (Table 3) were k_1 (0.001–1.5), k_0 (0.0005–0.5) and PERC (0–6).

Although the presupposed uniform priors overlap for the recession coefficients k_1 and k_0 , the ranges of their DREAM calibrated posteriors do not overlap for the HBV-Soil Parsim R and HBV-Parsim and do not overlap significantly for the other routines. This indicated that the DREAM calibration was able to constrain the model parameters to satisfy the conceptual representation of the quick runoff that is related to k_1 and the slow base flow that is related to k_0 . From the pure MC method, Seibert (1997a) and Uhlenbrook *et al.* (1999) found an overlap in k_1 and k_0 for some MC generated parameter sets, which is contradictory to the model conceptualisation. Even if there is a slight overlap between calibrated posterior ranges of k_2 and k_1 for the HBV-SMHI and k_1 and k_0 for the

HBV-non-linear, the parameter set corresponding to the maximum NSE and maximum NSELn complies with the conceptualisation of very quick runoff corresponding to k_2 , quick runoff corresponding to k_1 and slow baseflow corresponding to k_0 or $k_2 > k_1 > k_0$ (Table 6).

The strong negative correlations between the FC and the PERC parameters (Table 7) show the marked influence of parameterisations of the SM accounting on the runoff response parameters. As the FC increases, the relative saturation (SM/FC) decreases and hence the recharge decreases (based on the equation for the recharge in Table 2), which in turn reduces the percolation rate (related to the PERC parameter). For the HBV-non-linear, the negative correlations are more pronounced among the recession (drainage) coefficients and the non-linearity exponents of the outflow and baseflow equations showing existence of strong compensation or interaction among the recession coefficients and the non-linearity parameters. However, the results indicated positive correlation between the FC and the upper reservoir non-linearity coefficient. Generally, positive correlations were exhibited among the recession coefficient parameters and the PERC except for the HBV-SMHI, which showed very slight negative correlation between k_0 and PERC. Increase in the k_1 compensates for reduced storage in the upper reservoir as the PERC increases for simulation of outflow from the upper reservoir. Increase in PERC to increase the storage in the lower reservoir accompanied by an increase in k_0 favours generation of baseflow according to the baseflow equation.

CONCLUSIONS

We performed comparative evaluation of the four different configurations of the HBV runoff response routines (HBV-SMHI, HBV-non-linear, HBV-Soil Parsim R and HBV-Parsim). The results for the boreal catchments in mid-Norway indicated that the parsimonious conceptualisation (HBV-Parsim) with only five free parameters could extract the information content of the data efficiently with improved parameter identifiability. Also, better baseflow simulation was observed which complies with the high groundwater contribution to the streamflow for the study catchments as demonstrated in previous studies (Beldring

et al. 2000) and as guided by the baseflow separation techniques in the present study.

The findings of the study revealed the importance of comprehensive evaluation of parametrical parsimonious (i.e. small number of free parameters) simple linear storage–discharge relationships and the more complex HBV-based response routines. Further parsimony without compromising the quality of streamflow prediction could also be possible for snow-free or snow non-dominated catchments by excluding the snow routine. However, the more complex routines with a large number of reservoirs and parameters and linear and non-linear conceptualisations like the HBV-SMHI and HBV-non-linear may offer more flexibility for scientific research purposes (e.g., process understanding). However, increases in the number of parameters increases degrees of freedom and hence parameter unidentifiability problems, which in turn has negative implications for predictive uncertainty for operational purposes.

Usually only streamflow observation is readily available for parameter calibration, which is also usually the case for prediction for water management purposes. However, evaluations based on only the total streamflow are highly affected by the compensation and interacting effects among the storages and fluxes (outflows) of the upper and lower reservoirs. Therefore, the validity of the results of the conceptual HBV-based routines needs to be evaluated against their conceptualisation. Reliable prediction by the conceptual HBV models calls for evaluation of the internal simulation of the routines such as baseflow and possibly the SM state. For instance, the conceptualised simulated baseflow from the lower (ground water) reservoir should be compared against the baseflow estimated from other methods, e.g., baseflow separation techniques. To this end, development of proper baseflow separation techniques for the catchments would be necessary to evaluate the baseflow simulation of the HBV-based routines.

The findings should provide new information for the HBV users and the hydrological modelling community regarding the performances of different configurations of the conceptual HBV model. Equivalent performances of the HBV-Parsim indicated a potential for application of parametrical parsimonious models, which would benefit model updating for forecasting purposes. Evaluation of the routines based on a larger number of catchments (e.g.,

regional modelling) and for different climate regimes (e.g., Lidén & Harlin 2000), which requires availability of data and separate study, would be expected to provide further insights.

ACKNOWLEDGEMENTS

The research was supported by the Center for Environmental Design of Renewable Energy or CEDREN (<http://www.cedren.no>). We obtained the climate data from the Norwegian Meteorological Institute (<http://met.no/Klima>), Statkraft, TrønderEnergi and bioforsk (<http://www.bioforsk.no>). We obtained the streamflow data from the Norwegian Water Resources and Energy Directorate (<http://www.nve.no>). We also wish to thank the anonymous reviewers for their constructive comments, which helped to improve the manuscript.

REFERENCES

- Abebe, N. A., Ogden, F. L. & Pradhan, N. R. 2010 Sensitivity and uncertainty analysis of the conceptual HBV rainfall–runoff model: Implications for parameter estimation. *J. Hydrol.* **389**, 301–310.
- Bárdossy, A. & Singh, S. K. 2008 Robust estimation of hydrological model parameters. *Hydrol. Earth Syst. Sci.* **12**, 1273–1283.
- Bastola, S. & Murphy, C. 2013 Sensitivity of the performance of a conceptual rainfall-runoff model to the temporal sampling of calibration data. *Hydrol. Res.* **44** (3), 484–494.
- Beldring, S., Gottschalk, L., Rodhe, A. & Tallaksen, L. M. 2000 Kinematic wave approximations to hillslope hydrological processes in tills. *Hydrol. Process.* **14**, 727–745.
- Beldring, S., Engeland, K., Roald, L. A., Sælthun, N. R. & Vokso, A. 2003 Estimation of parameters in a distributed precipitation-runoff model for Norway. *Hydrol. Earth Syst. Sci.* **7** (3), 304–316.
- Bergström, S. 1976 *Development and application of a conceptual runoff model for Scandinavian catchments*. SMHI Reports RHO, No. 7, Norrköping.
- Beven, K. J. & Binley, A. M. 1992 The future of distributed models: Model calibration and uncertainty prediction. *Hydrol. Process.* **6**, 279–298.
- Beven, K. J. & Freer, J. 2001 Equifinality, data assimilation, and un-certainty estimation in mechanistic modelling of complex environmental systems using the GLUE methodology. *J. Hydrol.* **249**, 11–29.

- Blöschl, G., Reszler, C. & Komma, J. 2008 A spatially distributed flash flood forecasting model. *Environ. Modell. Softw.* **23**, 464–478.
- Booij, M. J. 2005 Impact of climate change on river flooding assessed with different spatial model resolutions. *J. Hydrol.* **303**, 176–198.
- Box, G. E. P. & Cox, D. R. 1964 An analysis of transformations. *J. R. Stat. Soc. B* **26**, 211–252.
- Clark, M. P. & Kavetski, D. 2010 The ancient numerical demons of conceptual hydrological modeling: 1. Fidelity and efficiency of time stepping schemes. *Water Resour. Res.* **46**, W10511.
- Das, T., Bárdossy, A., Zehe, E. & He, Yi. 2008 Comparison of conceptual model performance using different representations of spatial variability. *J. Hydrol.* **356**, 106–118.
- Driessen, T. L. A., Hurkmans, R. T. W. L., Terink, W., Hazenberg, P., Torfs, P. J. J. F. & Uijlenhoet, R. 2010 The hydrological response of the Ourthe catchment to climate change as modelled by the HBV model. *Hydrol. Earth Syst. Sci.* **14**, 651–665.
- Fenicia, F., Kavetski, D. & Savenije, H. H. G. 2011 Elements of a flexible approach for conceptual hydrological modeling: 1. Motivation and theoretical development. *Water Resour. Res.* **47**, W11510.
- Gardelin, M. & Lindström, G. 1997 Priestley-Taylor evapotranspiration in HBV-simulations. *Nord. Hydrol.* **28** (4–5), 235–246.
- Gelman, A. & Rubin, D. B. 1992 Inference from iterative simulation using multiple sequences. *Stat. Sci.* **7**, 457–472.
- Gupta, H. V., Beven, K. & Wagener, T. 2005 Model calibration and uncertainty estimation. *Encyclop. Hydrol. Sci.* **11** (131), 1–17.
- Harlin, J. 1991 Development of a process oriented calibration scheme for the HBV hydrological model. *Nord. Hydrol.* **22** (1), 15–36.
- Harlin, J. 1992 Modelling the hydrological response of extreme floods in Sweden. *Nord. Hydrol.* **23**, 227–244.
- Harlin, J. & Kung, C.-S. 1992 Parameter uncertainty and simulation of design floods in Sweden. *J. Hydrol.* **137**, 209–230.
- Hughes, D. A. 2010 Hydrological models: mathematics or science? Invited commentary. *Hydrol. Process.* **24**, 2199–2201.
- Hundecha, Y. & Bárdossy, A. 2004 Modeling of the effect of land use changes on the runoff generation of a river basin through parameter regionalization of a watershed model. *J. Hydrol.* **292**, 281–295.
- Jakeman, A. J. & Hornberger, G. M. 1993 How much complexity is warranted in a rainfall-runoff model? *Water Resour. Res.* **29** (8), 2637–2649.
- Kavetski, D. & Fenicia, F. 2011 Elements of a flexible approach for conceptual hydrological modeling: 2. Application and experimental insights. *Water Resour. Res.* **47**, W11511.
- Kavetski, D., Fenicia, F. & Clark, M. P. 2011 Impact of temporal data resolution on parameter inference and model identification in conceptual hydrological modeling: Insights from an experimental catchment. *Water Resour. Res.* **47**, W05501.
- Killingtveit, A. & Sælthun, N. R. 1995 *Hydropower development: Hydrology. Technical Report*, Norwegian Institute of Technology, Oslo.
- Kirchner, J. W. 2006 Getting the right answers for the right reasons: Linking measurements, analyses, and models to advance the science of hydrology. *Water Resour. Res.* **42**, W03S04.
- Kirchner, J. W. 2009 Catchments as simple dynamical systems: Catchment characterization, rainfall-runoff modeling, and doing hydrology backward. *Water Resour. Res.* **45**, W02429.
- Klemeš, V. 1986 Operational testing of hydrological simulation models. *Hydrolog. Sci. J.* **31**, 13–24.
- Kobold, M. & Brilly, M. 2006 The use of HBV model for flash flood forecasting. *Nat. Hazards Earth Syst. Sci.* **6**, 407–417.
- Kokkonen, T. S. & Jakeman, A. J. 2001 A comparison of metric and conceptual approaches in rainfall-runoff modeling and its implications. *Water Resour. Res.* **37** (9), 2345–2352.
- Kolberg, S. A. & Bruland, O. 2012 ENKI – An open source environmental modelling platform. Geophysical Research Abstracts 14, EGU2012-13630, EGU General Assembly.
- Kolberg, S. A. & Gottschalk, L. 2006 Updating of snow depletion curve with remote sensing data. *Hydrol. Process.* **20** (11), 2363–2380.
- Kolberg, S. A. & Gottschalk, L. 2010 Interannual stability of grid cell snow depletion curves as estimated from MODIS images. *Water Resour. Res.* **46**, W11555.
- Kuczera, G. & Mroczkowski, M. 1998 Assessment of hydrologic parameter uncertainty and the worth of multiresponse data. *Water Resour. Res.* **34** (6), 1481–1489.
- Lawrence, D., Haddeland, I. & Langsholt, E. 2009 *Calibration of HBV hydrological models using PEST parameter estimation*. Norwegian Water Resources and Energy Directorate Report, no. 1–2009.
- Li, H., Beldring, S. & Xu, C.-Y. 2014 Implementation and testing of routing algorithms in the distributed HBV model for mountainous catchments. *Hydrol. Res.* **45** (3), 322–333.
- Lidén, R. & Harlin, J. 2000 Analysis of conceptual rainfall-runoff modelling performance in different climates. *J. Hydrol.* **238**, 231–247.
- Lim, K. J., Engel, B. A., Tang, Z., Choi, J., Kim, K., Muthukrishnan, S. & Tripathy, D. 2005 *Web GIS-based hydrograph analysis tool, WHAT*. *J. Am. Water Resour. Assoc.* **41** (6), 1407–1416.
- Lindström, G. 1997 A simple automatic calibration routine for the HBV model. *Nord. Hydrol.* **28** (3), 153–168.
- Littlewood, I. G. & Croke, B. F. W. 2008 Data time-step dependency of conceptual rainfall-streamflow model parameters: An empirical study with implications for regionalization. *Hydrol. Sci. J.* **53** (4), 685–695.
- Merz, R., Parajka, J. & Blöschl, G. 2009 Scale effects in conceptual hydrological modeling. *Water Resour. Res.* **45**, W09405.
- Michaud, J. & Sorooshian, S. 1994 Comparison of simple versus complex distributed runoff models on a mid-sized semiarid watershed. *Water Resour. Res.* **30**, 593–605.
- Moreda, F., Koren, V., Zhang, Z., Reed, S. & Smith, M. 2006 Parameterization of distributed hydrological models: learning from the experiences of lumped modeling. *J. Hydrol.* **320**, 218–237.

- Nash, J. E. & Sutcliffe, J. V. 1970 River flow forecasting through conceptual models, I. A discussion of principles. *J. Hydrol.* **10**, 228–290.
- Nathan, R. J. & McMahon, T. A. 1990 Evaluation of Automated Technique for BaseFlow and Recession analyses. *Water Resour. Res.* **26** (7), 1465–1473.
- Pechlivanidis, I. G., Jackson, B. M., Mcintyre, N. R. & Wheeler, H. S. 2011 Catchment scale hydrological modelling: a review of model types, calibration approaches and uncertainty analysis methods in the context of recent developments in technology and applications. *Global NEST J.* **13** (3), 193–214.
- Perrin, C., Michel, C. & Andréassian, V. 2001 Does a large number of parameters enhance model performance? Comparative assessment of common catchment model structures on 429 catchments. *J. Hydrol.* **242**, 275–301.
- Priestley, C. H. B. & Taylor, R. J. 1972 On the assessment of surface heat flux and evaporation using large-scale parameters. *Mon. Weather Rev.* **100**, 81–82.
- Rakovec, A., Weerts, H., Hazenberg, P., Torfs, P. J. J. F. & Uijlenhoet, R. 2012 State updating of a distributed hydrological model with ensemble Kalman filtering: effects of updating frequency and observation network density on forecast accuracy. *Hydrol. Earth Syst. Sci.* **16**, 3435–3449.
- Reed, S., Koren, V., Smith, M., Zhang, Z., Moreda, F. & Seo, D.-J. 2004 DMIP participants. overall distributed model intercomparison project results. *J. Hydrol.* **298**, 27–60.
- Sæthun, N. R. 1996 *The 'Nordic' HBV model. Description and documentation of the model version developed for the project climate change and energy production.* Publication No. 7. Norwegian Water Resources and Energy Administration, Hydrology Department, Oslo.
- Samuel, J., Coulibaly, P. & Metcalfe, R. A. 2011 Estimation of continuous streamflow in Ontario ungauged basins: Comparison of regionalization methods. *J. Hydrol. Eng.* **16** (5), 447–459.
- Schoups, G. & Vrugt, J. A. 2010 A formal likelihood function for parameter and predictive inference of hydrologic models with correlated, heteroscedastic, and non-Gaussian errors. *Water Resour. Res.* **46**, W10531.
- Seibert, J. 1997a Estimation of parameter uncertainty in the HBV model. *Nord. Hydrol.* **28** (4–5), 247–262.
- Seibert, J. 1997b HBV light version 1.2. *User's manual.* Uppsala University, Department of Earth Science, Hydrology, Uppsala.
- Seibert, J. 2000 Multi-criteria calibration of a conceptual runoff model using a genetic algorithm. *Hydrol. Earth Syst. Sci.* **4** (2), 215–224.
- Seibert, J. 2002 *HBV light version 2, User's manual,* Environmental Assessment, SLU, Uppsala.
- Seibert, J. 2003 Reliability of model predictions outside calibration conditions. *Nord. Hydrol.* **34** (5), 477–492.
- Shrestha, D. L. & Solomantine, D. P. 2008 Data-driven approaches for estimating uncertainty in rainfall-runoff modelling. *Int. J. River Basin Manage.* **6** (2), 109–122.
- Shrestha, D. L., Kayastha, N. & Solomatine, D. P. 2009 A novel approach to parameter uncertainty analysis of hydrological models using neural networks. *Hydrol. Earth Syst. Sci.* **13**, 1235–1248.
- Sicart, J. E., Pomeroy, J. W., Essery, R. L. H. & Bewley, D. 2006 Incoming longwave radiation to melting snow: observations, sensitivity and estimation in northern environments. *Hydrol. Process.* **20**, 3697–3708.
- Smith, M. B., Seo, D.-J., Koren, V. I., Reed, S. M., Zhang, Z., Duan, Q., Moreda, F. & Cong, S. 2004 The distributed model intercomparison project (DMIP): motivation and experiment design. *J. Hydrol.* **298**, 4–26.
- Sorman, A. A., Sensoy, A., Tekeli, A. E., Sorman, A. & Akyurek, U. Z. 2009 Modelling and forecasting snowmelt runoff process using the HBV model in the eastern part of Turkey. *Hydrol. Process.* **23**, 1031–1040.
- Teuling, J., Lehner, I., Kirchner, J. W. & Seneviratne, S. I. 2010 Catchments as simple dynamical systems: Experience from a Swiss prealpine catchment. *Water Resour. Res.* **46**, W10502.
- Uhlenbrook, S., Seibert, J., Leibundgut, C. & Rodhe, A. 1999 Prediction uncertainty of conceptual rainfallrunoff models caused by problems in identifying model parameters and structure. *Hydrolog. Sci. J.* **44** (5), 779–797.
- van den Tillaart, S. P. M. 2010 Influence of uncertainties in discharge determination on the parameter estimation and performance of a HBV model in Meuse sub basins Enschede. April 2010, Master Thesis, Water Engineering & Management University of Twente, The Netherlands.
- van Werkhoven, K., Wagener, T., Reed, P. M. & Tang, Y. 2009 Sensitivity-guided reduction of parametric dimensionality for multi-objective calibration of watershed models. *Adv. Water Resour.* **32** (8), 1154–1169.
- Vrugt, J. A. & Ter Braak, C. J. F. 2011 DREAM(D): an adaptive Markov chain Monte Carlo simulation algorithm to solve discrete, noncontinuous, and combinatorial posterior parameter estimation problems. *Hydrol. Earth Syst. Sci.* **15**, 3701–3713.
- Vrugt, J. A., Bouten, W., Gupta, H. V. & Sorooshian, S. 2002 Toward improved identifiability of hydrologic model parameters: The information content of experimental data. *Water Resour. Res.* **38** (12), 1312, doi:10.1029/2001WR001118.
- Vrugt, J. A., Ter Braak, C. J. F., Diks, C. G. H., Robinson, B. A., Hyman, J. M. & Higdon, D. 2009 Accelerating Markov Chain Monte Carlo simulation by differential evolution with self-adaptive randomized subspace sampling. *J. Nonlinear Sci. Numer. Simul.* **10** (3), 273–290.
- Vrugt, J. A., Ter Braak, C. J. F., Diks, C. G. H. & Schoups, G. 2013 Hydrologic data assimilation using particle Markov chain Monte Carlo simulation: Theory, concepts and applications. *Adv. Water Resour.* **51**, 457–478.
- Wagener, T., Freer, J., Zehe, E., Beven, K., Gupta, H. & Bárdossy, A. 2005 Towards an uncertainty framework for predictions in ungauged basins: The Uncertainty Working Group. In: *Predictions in Ungauged Basins: Promise and Progress* (M. Sivapalan, T. Wagner, S. Uhlenbrook, X. Liang, V. Lakshmi, P. Kumar, E. Zehe & Y. Tachikawa, eds). IAHS Publication 303, Wallingford.

- Wang, Y., He, B. & Takase, K. 2009 Effects of temporal resolution on hydrological model parameters and its impact on prediction of river discharge. *Hydrol. Sci. J.* **54** (5), 886–898.
- Willems, P. 2009 A time series tool to support the multi-criteria performance evaluation of rainfall-runoff models. *Environ. Modell. Softw.* **24**, 311–321.
- Winsemius, H. C., Schaefli, B., Montanari, A. & Savenije, H. H. G. 2009 On the calibration of hydrological models in ungauged basins: A framework for integrating hard and soft hydrological information. *Water Resour. Res.* **45**, W12422.
- Wrede, S., Seibert, J. & Uhlenbrook, S. 2013 Distributed conceptual modelling in a Swedish lowland catchment: a multi-criteria model assessment. *Hydrol. Res.* **44** (2), 318–333.
- Zięba, A. 2010 Effective number of observations and unbiased estimators of variance for autocorrelated data an overview. *Metrol. Meas. Syst.* **XVII** (1), 3–16.

First received 5 March 2014; accepted in revised form 9 July 2014. Available online 12 August 2014